Impact of landscape pattern change on runoff processes in catchment area of the Ulungur River Basin

Fan Gao, Bing He, Songsong Xue and Yizhen Li

ABSTRACT

Based on the Soil and Water Assessment Tool (SWAT) model, the monthly runoff processes of two land-use types in 2000 and 2015 were simulated in this paper. The relationship between runoff and landscape pattern was analyzed, and the spatial correlation between runoff and landscape pattern analyzed using the geographic weighted regression model combined with the change of landscape pattern in the study area from 2000 to 2015. The results show the following. (1) The SWAT model can simulate the monthly runoff processes in the catchment area of the Ulungur River Basin (URB) under different land-use types for 2000 and 2015, but the simulation effect in 2000 was found to be better than that in 2015. (2) From 2000 to 2015, the area of woodland and grassland decreased. Runoff was positively correlated with woodland, grassland, largest patch index, mean patch area (AREA_MN), and contagion index, and negatively correlated with others. This indicates that the landscape fragmentation of URB was aggravated in 2000–2015, the landscape balance was destroyed, and the ability of rainfall interception and water conservation was weakened. (3) Landscape pattern indicators of grassland had a negative spatial impact on URB runoff, and the northern region of URB was more severely affected in 2015 than in 2000. AREA_MN landscape pattern index had a positive impact on runoff in the northern part of URB, and the positive impact in northern URB in 2000 was better than that in 2015.

Key words | CMADS, landscape pattern, runoff processes, SWAT model, Ulungur River

Fan Gao
Songsong Xue
Yizhen Li
Water Conservancy and Civil Engineering College,
Xinjiang Agricultural University,
Urumqi, Xinjiang, 830052,
China

Bing He (corresponding author)
State Key Laboratory Base of Eco-Hydraulics in Northwest Arid Region of China,
Xi'an University of Technology,
Xi'an 710048,
China
E-mail: *bing_touch_he@163.com*

INTRODUCTION

Landscape pattern is a spatial arrangement of landscape patches of different sizes, shapes, and types. It is the result of the coupling of various human activities and natural factors at different scales (Zhang & Zeng 2018). Landscape pattern changes affect a series of ecological and hydrological processes such as water cycle and biogeochemical cycle of the terrestrial ecosystem. It is mainly reflected in the spatial and temporal changes of land use and surface cover, as well as its influence on the formation of hydrological processes such as surface evapotranspiration, interception, sink filling, soil water infiltration, and groundwater, which leads to changes in the runoff generation and confluence process, and further affects the hydrological cycle and water resource cycle process with land as underlying surface (Wang *et al.* 2006; Dong *et al.* 2012; Tian *et al.* 2019). Since the 20th century, with the continuous enhancement of human activities and the rapid development of economy and society, large-scale farmland reclamation, urban and water conservancy projects have changed the landscape pattern of basins. This has a significant impact on the formation, transformation, and spatial and temporal distribution of water resources in basins, which leads to a series of water-related ecological and environmental problems such as soil erosion and frequent occurrence of the extreme hydrological events (Li *et al.* 2013). Therefore, the study of hydrological response to

doi: 10.2166/ws.2020.027

landscape pattern changes has become a hot and frontier issue in global ecological and environmental researches in recent years, and it has important practical significance and scientific value for watershed water resources management and revealing the regional and global hydrological cycle law (Foley *et al.* 2005; Li *et al.* 2007).

At present, research on the hydrological effects of human activities mainly focus on the effects on runoff (Gao *et al.* 2009; Dong *et al.* 2012), and the methods include the time series method of hydrological characteristic parameters, the experimental watershed method, and the hydrological model simulation method of watershed. The time series method of hydrological characteristic parameters, due to short data time series and insufficient observation density, cannot reflect the effect mechanisms of watershed spatial heterogeneity and landscape pattern changes on hydrological processes, and it is difficult to establish a clear correlation between landscape pattern and runoff (Dong *et al.* 2012; Wang *et al.* 2016). The experimental watershed method can only be applied to the small watershed where the geographical and meteorological conditions are basically the same, but not to the large meso-scale watershed where the topographical, geomorphic, and climatic conditions have significant differences. The simulation method of watershed hydrological model, which takes into account the spatial differences of geographical factors, can effectively simulate the complex hydrological cycle in nature (Xu & Cheng 2010; Sriwongsitangon & Taesombat 2011). Therefore, the runoff effect of landscape pattern changes can be effectively analyzed by constructing watershed hydrological models, especially the distributed hydrological models based on physical basis. Compared with other hydrological models, the Soil and Water Assessment Tool (SWAT) model has a strong physical mechanism and has been widely used to simulate the hydrological response of watershed in the context of land use/cover change (LUCC) and climate change (Ghaffari *et al.* 2010; Wang *et al.* 2016).

Ulungur River, the second largest river in the Altay region of Xinjiang, China, is a typical arid inland river, located at the northwest edge of the Dzungaria Basin, and its water source comes from seasonal snow melt and precipitation supply from water catchment. In recent years, the Ulungur River catchment area has been affected by high-intensity human activities, leading to the variation of regional runoff sequence, and a series of water-related ecological and environmental problems such as natural vegetation degradation and soil erosion (Nurland *et al.* 2014; He *et al.* 2019). Therefore, the study of the impact of landscape pattern changes on runoff in this region has both theoretical and practical significance for guaranteeing the water ecological security of this region and promoting the rational development, utilization, and protection of soil and water resources. As for the runoff simulation of the Ulungur River Basin, Yang (2014) had constructed a distributed hydrological model based on the SWAT model, and discussed the applicability of the SWAT model in the Ulungur River and the impact of climate change on the runoff from the Ulungur River. However, no analysis has been made on the response mechanism of runoff to landscape pattern changes in this region.

On this basis, based on the SWAT model driven by China Atmospheric Assimilation Driven Data Set (CMADS) which was established by Meng (Meng 2016; Meng *et al.* 2016), the monthly runoff process under the two land-use types in 2000 and 2015 and the meteorological conditions from 2008 to 2015 were simulated, respectively. The relationship between runoff and landscape pattern was analyzed through the changes of landscape pattern types and landscape indices at a landscape level in the study area from 2000 to 2015. The appropriate landscape pattern indices were selected, and the spatial correlation between runoff and landscape pattern was analyzed by the geographical weighted regression (GWR) model to explore the response mechanism between runoff and landscape pattern change, thus providing scientific basis for the rational development and utilization of soil and water resources and the formulation of water environmental protection policy in this basin.

Study area and data

The Ulungur River originates from the Qinggeli River in Qinghe county, Altay region, Xinjiang, China. The river consists of two first-grade tributaries (Qinggeli River,

Burrgen River) and four second-grade tributaries (Daqinggeli River, Xiaoqinggeli River, Qianghan River, and Chagangule River). The Ulungur River Basin (89°47′E–91°04′E, 45°00′N–47°20′N) has a border with Mongolia in the east and north, and is adjacent to the Fuyun county and the Changji Hui Autonomous Prefecture in the west, and the Gurbantunggute Desert in the south (Kang *et al.* 2018). The catchment area of Ulungur River Basin (this paper refers to the catchment area above the Ertai Hydrologic Station at the mountain-pass, hereinafter referred to as URB) is $1.84 \times 10^4\,km^2$ (in China), accounting for about 32% of the total area, and the average annual runoff is $9.87 \times 10^8\,m^3$. The river recharge comes from seasonal snow melt water and precipitation in mountainous areas (Yang 2014). Located in the center of the Eurasia, the URB is a typical Dzungaria arid zone, with dry and windy springs, hot summers, cool autumns, and long cold winters. As it is far away from the ocean, it is difficult for sea water vapor to enter the basin. Surrounded by mountains, the region not only blocks the water vapor from entering, but also intercepts a large amount of water vapor, so the mountainous area is the runoff generating area of the basin. The Ulungur River Basin has an annual average precipitation of 129.8 mm (precipitation increases with elevation), an annual average temperature of 3.9 °C (high temperature mainly occurs in June to August), and an annual average potential evaporation of 867.2 mm (Nurland 2014; Yang 2014; He *et al.* 2019).

Data

The input data of the SWAT model include spatial distribution data, such as the Digital Elevation Model (DEM), LUCC data, soil type, and attribute data such as meteorological data and measured runoff data. Among them, Shuttle Radar Topography Mission (SRTM) 90 DEM was selected for the data elevation model, which was derived from DEM data in SRTM format (http://srtm.csi.cgiar.org/SELECTION/inputcoord.asp) of NASA's website, with a resolution of $90 \times 90\,m^2$. Land-use data include two issues of Landsat series remote sensing image data thematic maps from 2000 and 2015. The remote sensing images were derived from geospatial data cloud (http://www.gscloud.cn/), with a resolution of $30 \times 30\,m^2$. The soil data were extracted from the China Soil Data Set (v1.0) of the World Soil Database. The main fields of the soil attribute table are the FAO 90 soil classification system, soil reference depth, soil physics (volume percentage of gravel, clay content of sand powder, effective water content, etc.), and chemical properties (organic carbon content, cation exchange capacity, etc.). The meteorological data were obtained from CMADS (Meng 2016; Meng *et al.* 2016). The runoff data were selected from the monthly measured runoff data from 2008 to 2015 of the Ertai hydrologic stations in the source area of the Ulungur River Basin, which were obtained from the Hydrological and Water Resources Survey Bureau of Altay, Xinjiang, China. In order to maintain the consistency of resolution of the SWAT model, the resolutions of DEM, LUCC, soil, and other spatial data were unified to 1 km, and the projection coordinate system was uniformly set as Bejing_1954_GK_Zone_17N.

METHODOLOGY

Construction of the SWAT model

The SWAT model can simulate the hydro-physical processes of river basins over a long period of time, including the transport and transformation of water, sediment, chemical substances, etc. based on the principle of water balance equation and the spatial data information provided by the geographic information system (GIS) and remote sensing (RS) software (Ghaffari *et al.* 2010; Lv *et al.* 2018; Hou & Gao 2019). In this study, the SWAT model 2009 was adopted to calibrate and verify the runoff data measured by the Ertai Hydrological Station in the Ulungur River Basin mountain-pass based on the ArcGIS 9.3 software platform to simulate the runoff in the source area of the URB. On the basis of previous research results (Yang 2014), the area of the minimum catchment threshold was set at 18,630 hm^2, and the study area was divided into 19 sub-basins with consideration of the actual watershed and sub-basin division significance. Based on slope gradients the study area was divided into four segments <10%, 10–30%, 30–45%, >45%. At the same time, the land-use, soil, and gradient control thresholds were set to 10%, 10% and 20%, respectively.

Finally, the whole study area was divided into 151 hydrological response units. The model was calibrated and verified on a monthly time scale by taking 2008–2009 as the model warm-up period, 2010–2013 as the rate period, and 2014–2015 as the verification period. The sensitivity analysis module of Latin Hypercube One-factor-At-a-Time (LH-OAT), which comes with the SWAT model, was used for parameter sensitivity analysis and parameter calibration. The Nash–Sutcliffe efficiency coefficient (*Ens*) and the determination coefficient (R^2) were selected as evaluation indices to measure the efficiency of the model, and the specific calculation formula was based on Popov (1979), where when $Ens > 0.75$ and $R^2 > 0.6$, it means that the simulation results of the model are very good.

With the calibrated model and other parameters unchanged, the meteorological data of the CMADS data set from 2008 to 2015 and the land-use data of 2000 and 2015 were loaded to simulate the two monthly runoff processes (different land-use types in 2000 and 2015) under the meteorological conditions of 2008–2015. The two simulation results were then compared to explore the impact of landscape pattern changes on runoff.

Selection of landscape indices

Landscape indices highly condense the information of landscape pattern, which can reflect its structure and spatial distribution characteristics, and thus better explain and reflect the landscape function (Guo *et al*. 2018). Landscape indices can be divided into patch-metric, class-metric, and landscape-metric. In this study, the results of land-use type extraction in 2000 and 2015 were taken as the landscape composition types of the study area. Based on the actual situation of the study area, the landscape pattern indices were calculated using the landscape pattern analysis software Fragstats3.3. Eight landscape pattern indices at the landscape level were determined, namely number of patches (NP), patch dens (PD), largest patch index (LPI), landscape shape index (LSI), mean patch area (AREA_MN), contagion index (CONTAG), Shannon's diversity index (SHDI), and Shannon's evenness index (SHEI). These landscape pattern indices mainly reflect the area of each landscape type, fragmentation degree of landscape type, complexity of landscape shape, landscape balance, and landscape connectivity in the study area. Landscape indices of 19 sub-basins in URB in 2000 and 2015 were counted, and the change rates of landscape pattern in 2000–2015 were calculated for the whole basin and 19 sub-basins, respectively. The formula is as follows:

$$R_m = \frac{K_{m,2015} - K_{m,2000}}{K_{m,2000}} \times 100\% \quad (1)$$

where R_m is the change rate of m-type landscape pattern indices, $K_{m,2015}$ is the value of m-type landscape pattern indices at the level of landscape in 2015, and $K_{m,2000}$ is the value of m-type landscape pattern indices at the level of landscape in 2000.

Analysis of correlation between landscape pattern change and runoff change

The Pearson correlation analysis method was used to calculate the correlation between the change rate of landscape pattern indices and runoff in 19 sub-watersheds under two landscape types in 2000 and 2015 based on the Statistical Product and Service Solutions software in order to analyze the impact of landscape pattern change on runoff. By comparing and analyzing the results of correlation between the change rate of landscape pattern indices and runoff, the landscape indices (which were independent of each other and had a greater impact on runoff) were selected to analyze the spatial impact of landscape pattern index on runoff distribution.

The GWR model

The GWR model is a local spatial analysis method proposed by Brunsdon *et al*. based on the traditional regression model (Brunsdon *et al*. 1996; Hou & Gao 2019). The model incorporates the spatial location of data into the parameters, and evaluates the spatial variation of the relationship between independent variables and dependent variables by obtaining local parameters. Referring to the previous research results (Hou & Gao 2019), the Gaussian kernel function was selected as the kernel function of the model, and the Akaike information criterion (AIC) criterion method was selected to determine the optimal bandwidth.

The accuracy of the model was tested by the AI value (if the difference of AI values between the two models is greater than three, the model with the lower AI values will be considered a better model), and the GWR model was used to reveal the spatial relationship between runoff and landscape pattern indices in different years under spatial non-stationary conditions. The specific expression of the GWR model is as follows:

$$y_i = \beta_0(\mu_i, \vartheta_i) + \sum_{j=1}^{k} \beta_k(\mu_i, \vartheta_i) x_{ik} + \varepsilon_i \quad (2)$$

where (μ_i, ϑ_i) represents the coordinates of the ith sampling point; k is the number of independent variables; y_i, x_{ik}, and ε_i respectively represent independent variables (runoff), dependent variables (landscape pattern index) of regression point i, and random error terms conforming to normal distribution; $\beta_0(\mu_i, \vartheta_i)$ represents the intercept of the GWR model at regression point i; and $\beta_k(\mu_i, \vartheta_i)$ refers to the slope of the GWR model at regression point i. The parameters can be estimated by the following formula:

$$\beta(\mu_i, \vartheta_i) = (X^T W(\mu_i, \vartheta_i)\mathrm{X})^{-1} X^T W(\mu_i, \vartheta_i)^Y \quad (3)$$

where $\beta(\mu_i, \vartheta_i)$ represents unbiased estimation of regression coefficients and $W(\mu_i, \vartheta_i)$ represents spatial weight matrix, which is the core of GWR. The closer the observation point is to a specific point, the greater the weight. X and Y represent the matrix of independent and dependent variables, respectively. The weight function of Gauss space has universality and its expression is as follows:

$$\omega_{ij} = \exp\left(-\frac{d_{ij}^2}{b^2}\right) \quad (4)$$

where ω_{ij} denotes the weight of observation point j; d_{ij} denotes the Euclidean distance between the regression point i and the observation point j around I; and b denotes the non-negative attenuation parameter of the functional relationship between weight and distance, also known as bandwidth. When the distance between observation points is larger than the b value, the weight tends to zero rapidly.

RESULTS AND ANALYSIS

Calibration and verification of runoff simulation based on the SWAT model

According to the relative sensitivity of model parameters and combined with previous research results (Yang 2014), eight parameters of the model were determined. Referring to the physical meaning of each parameter and the actual situation of the study area, the parameters were adjusted manually until the simulation values were close to the measured values. Finally, the range of parameters was determined as shown in Table 1. The *Ens* and the correlation coefficient R^2 were used to evaluate the

Table 1 | Final value range of sensitivity parameters

Parameter	Description	Value range		Calibrated value	Sensitivity order
		Min	Max		
CN2	Initial soil conservation service runoff curve number to moisture conditions II	35	98	95	1
SOL_AWC	Effective water capacity of soil layer (mmH_2O/mm soil)	0	1	0.01	2
ALPHA_BF	Baseflow regression constant (days)	0	1	0.21	3
ESCO	Soil evaporation compensation coefficient (mm/h)	0	1	0.89	4
CH_K2	Effective hydraulic conductivity (mm/h)	0	150	125	5
GW_REVAP	Groundwater 'revap' coefficient	−1	1	−0.73	6
REVAPMN	Threshold of evaporation in shallow aquifer	−100	100	55	7
SOL_K	Soil hydraulic conductivity (mm/h)	−25	25	5	8

Table 2 | The monthly runoff calibration and verification results of the Ertai Hydrological Station under different land-use types

	Calibration period (2010–2013)		Validation period (2014–2015)	
Land-use types	***Ens***	R^2	***Ens***	R^2
2000	0.81	0.96	0.86	0.90
2015	0.79	0.96	0.84	0.90

applicability of the model in the study area, the process lines of comparison between the measured and simulated monthly runoff rates from the Ertai Hydrological Station under the conditions of land-use type (or landscape type) in 2000 and 2015 and the applicability evaluation results (Table 2) were obtained (see Figure 1). Table 2 shows that the monthly runoff from the Ertai Hydrological Station in the verification period of 2000 and 2015 was in good agreement with the measured values, and the evaluation indices met the requirements (when $Ens > 0.75$, $R^2 > 0.6$). This indicates that the results of model simulation under different land-use types (or landscape types) in 2000 and 2015 were good, and it also indicates that the use of the CMADS data set to drive the SWAT model for the URB runoff simulation had a good applicability, and can be used to study the spatial impact of landscape pattern changes on the monthly runoff from the URB. Simultaneously, as can be seen from Figure 1 and Table 2, the *Ens* coefficients of the Ertai Hydrological Station in 2000 were slightly higher than those in 2015, indicating that the monthly runoff simulated by the model under land-use type (or landscape type) in 2000 was slightly better than that in 2015, that is, the average monthly runoff from the URB under land-use input in 2015 was 8.9% less than that in 2000.

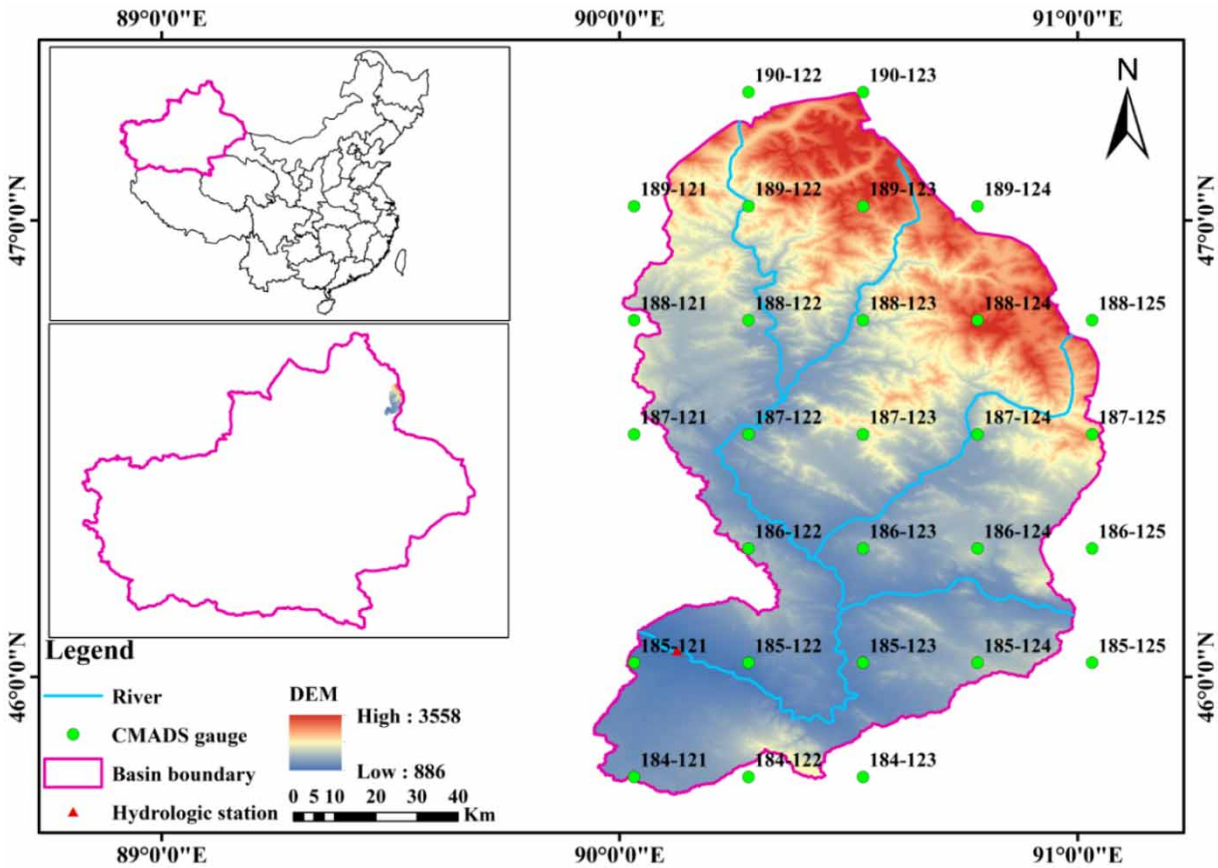

Figure 1 | The geographical map of the study area.

Analysis of landscape pattern change

Area change of landscape types

The area changes of landscape types in the two periods of 2000 and 2015 are shown in Table 3. It can be seen that bare land was the main landscape type in the two periods, with an area of 4,898.89 km^2 in 2000 and 4,923.82 km^2 in 2015, accounting for 51.03% and 51.29% of the total URB area, followed by grassland and woodland, accounting for 32.39% and 12.49% in 2000, 32.75% and 11.30% in 2015, respectively. The proportion of cultivated land, water area, and construction land landscape types in the two periods was relatively small. During 2000–2015, the landscape types of the URB were mainly woodland and grassland and their area showed a decreasing trend during this period, decreasing by 83.64 km^2 and 25.95 km^2, respectively. Combined with Figure 2, it can be seen that the reduced area of woodland was mainly transformed into grassland and the reduced area of grassland was mainly transformed into bare land and cultivated land. The cultivated land, water area, construction land, and bare land were all increasing by 40.21 km^2, 30.50 km^2, 3.92 km^2, and 34.94 km^2, respectively. It can be seen from Figure 2 that the increased area of cultivated land mainly came from the transformation of bare land and grassland.

Change of landscape indices at landscape level

The results of the landscape level indices calculation in the URB are shown in Table 4. It can be seen that the NP increased from 4,448 to 4,781 and the PD increased from 0.47 to 0.51 in 2000–2015, which indicated that the degree of landscape fragmentation was increasing. The CONTAG showed a decreasing trend from 54.15% in 2000 to 53.19% in 2015, indicating that the connectivity of landscape patches decreased, the large patches were divided into scattered small patches, and the degree of landscape fragmentation increased. The LPI, AREA_MN decreased, and the LSI, SHDI, and the SHEI increased from 2000 to 2015, which indicated that the area differences of the URB landscape types decreased, landscape spatial structure diversified, landscape complexity increased, heterogeneity enhanced, and dominance decreased. This shows that the disturbance degree of human activities to landscape types was increasing, which also shows that the landscape status of forest land and grassland was declining, the landscape status of cultivated land and construction land was rising, and the level of urbanization was constantly increasing.

Analysis of correlation between runoff and landscape pattern

The correlation between runoff change rate and landscape pattern indices change rate was analyzed using the Pearson correlation analysis, and the relationship between landscape pattern and runoff was quantitatively analyzed using statistics of the area changes of each landscape type, landscape indices change at landscape level, and the runoff change simulated by the SWAT model in 19 sub-basins from 2000 to 2015. The results are shown in Tables 5 and 6. From the runoff response of landscape

Table 3 | Landscape type area changes in the URB in 2000 and 2015

	2000		2015			
Landscape types	**Area (km^2)**	**Proportion (%)**	**Area (km^2)**	**Proportion (%)**	**Area of change (km^2)**	
Framland	132.08	1.38	172.29	1.79	40.21	30.44
Woodland	1,088.76	11.34	1,005.13	10.47	−83.64	−7.68
Grassland	3,129.63	32.60	3,103.69	32.33	−25.95	−0.83
Water	27.38	0.29	57.88	0.60	30.50	111.44
Construction land	13.27	0.14	17.19	0.18	3.92	29.51
Bare land	5,008.88	52.18	5,043.82	52.54	34.94	0.70

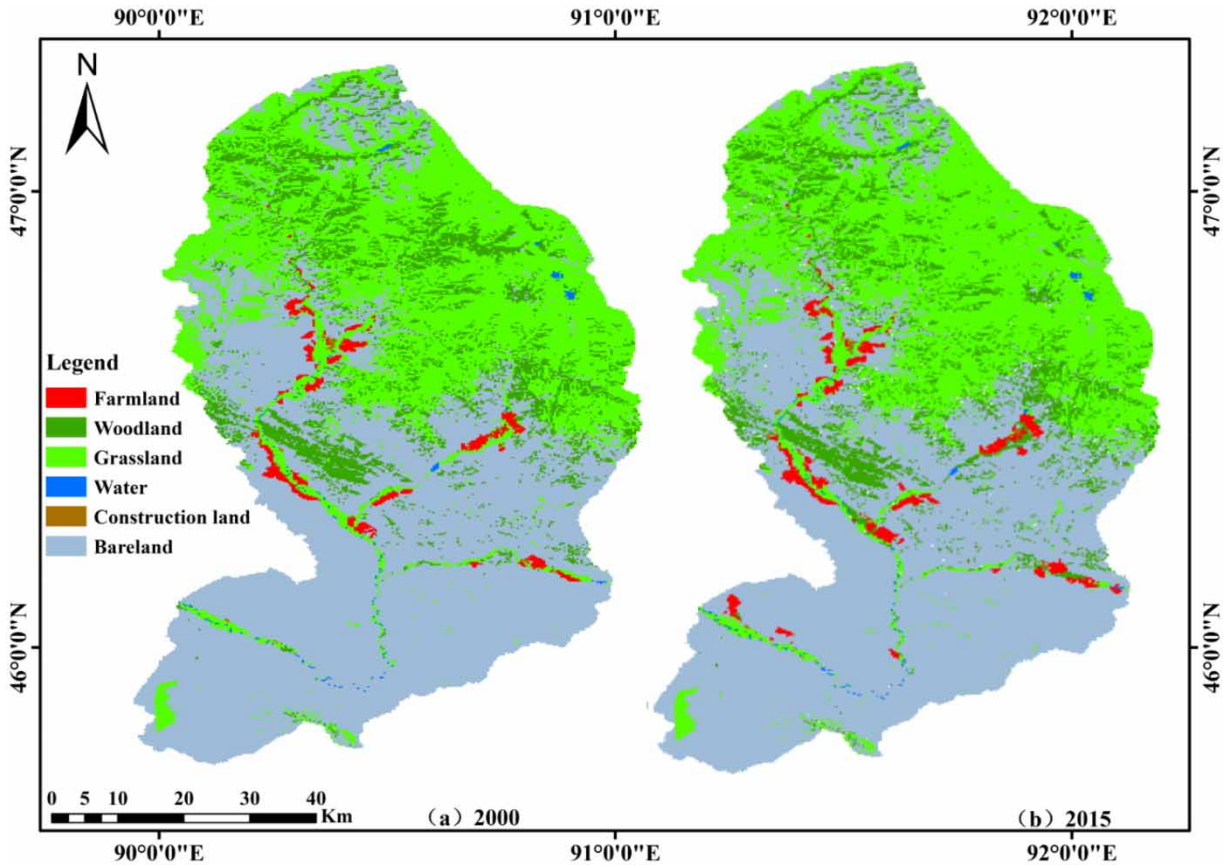

Figure 2 | Thematic maps of land-use types in the study area in 2000 and 2015.

Table 4 | Landscape level index change analysis in the URB in 2000 and 2015

Landscape metrics	NP	PD	LPI	LSI	AREA_MN	CONTAG	SHDI	SHEI
2000	4,448	0.47	42.60	28.20	211.36	54.15	1.034	0.58
2015	4,781	0.51	41.70	29.3	196.15	53.19	1.06	0.59

Table 5 | Analysis of the correlation between runoff change and landscape type change

	Landscape type change					
	Farmland	Woodland	Grassland	Water	Construction land	Bare land
Runoff change	−0.707[a]	0.407[a]	0.579[a]	0.279	−0.473[b]	−0.379

[a]Significant correlation at 0.01 level (bilateral).
[b]Significant correlation at 0.05 level (bilateral).

type area change, the runoff change and woodland, grassland and water landscape area change were all positively correlated, indicating that runoff would decrease with an decrease in these landscape type areas, and vice versa. The correlation coefficients between runoff and forest land and grassland were 0.407 and 0.579, respectively,

Table 6 | Analysis of the correlation between runoff change and landscape pattern index change

	Landscape type change							
	NP	PD	LPI	LSI	AREA_MN	CONTAG	SHDI	SHEI
runoff change	−0.733**	−0.730	0.434	−0.569*	0.805**	0.273	−0.684**	−0.556*

** indicates significant correlation at 0.01 level (bilateral).
* indicates significant correlation at 0.05 level (bilateral).

and both passed the significance level requirements of 0.01 and 0.05, indicating that the decrease of forest land and grassland from 2000 to 2015 would reduce the water conservation capacity of the study area, which was not conducive to the formation of runoff. The correlation coefficient between runoff and water was 0.279, indicating that the increase of water area can accelerate the speed of runoff confluence, thus increasing the runoff. The runoff change was negatively correlated with the change of cultivated land, construction land, and bare land landscape area, indicating that runoff would decrease with an increase in these landscape types, and vice versa. The negative correlation coefficients between runoff and cultivated land, construction land, and bare land were 0.707, 0.473, and 0.379, respectively. It indicates that the increase of cultivated land, construction land, and bare land from 2000 to 2015 weakened the surface interception of precipitation and increased the infiltration capacity of precipitation, thus affecting the hydrological situation and the runoff generation and confluence mechanisms of the study area.

From the correlation between runoff change and landscape index change at landscape level, the runoff change was positively correlated with changes in LPI, AREA_MN, and CONTAG, with correlation coefficients of 0.434, 0.805, and 0.273 respectively. Among them, only the correlation between runoff change and AREA_MN passed the significance level requirements of 0.01 and 0.05. The results show that the changes of the three landscape indices from 2000 to 2015 have an impact on runoff, especially the AREA_MN. Compared with the landscape pattern in 2000, the landscape connectivity in the URB in 2015 was worse, patch shape complexity was increased, landscape fragmentation was aggravated, which weakened the ability of rainfall interception and water conservation in the study area, and made runoff decrease. Runoff changes were negatively correlated with NP, PD, LSI, SHDI, and SHEI. Moreover, the correlation between runoff change and change in these indices all passed the significance level requirements (0.01 and 0.05), indicating that from 2000 to 2015, the disturbance of human activities on landscape types during the transformation of forest and grassland landscape in the URB to cultivated land, construction land, and bare land landscape resulted in the destruction of landscape equilibrium, the diversification of spatial structure and the enhancement of heterogeneity, which led to the deterioration of rainfall interception capacity and runoff decreasing in the study area.

Spatial correlation between runoff and landscape pattern

According to the correlation analysis of runoff and landscape pattern, it can be seen that runoff was significantly correlated with farmland, woodland, grassland and NP, AREA_MN, and SHDI in landscape pattern indices. Therefore, based on the GWR model, the spatial correlation between runoff (the dependent variables) and the six landscape pattern indices (the independent variables) at the sub-basin scale was analyzed. The premise of using the GWR model is that the spatial correlation among variables does exist, and the Moran's *I* index was used to pre-test the spatial correlation of the six landscape pattern indices before modeling and analysis. The spatial statistics tool of the ArcGIS 9.3 software was used for calculation (see Table 7). It can be seen that only the Moran's *I* value of grassland and AREA_MN was greater than 0, and it passed the significance test of 95% confidence level, indicating that grassland and AREA_MN in landscape pattern indices had strong clustering pattern characteristics in space.

Finally, two landscape pattern indices, grassland and AREA_MN, were selected as independent variables for

Table 7 | Spatial correlation eigenvalues of landscape pattern indices in the URB

	2000		2015	
Landscape pattern index	**Moran's *I***	***p* value**	**Moran's *I***	***p* value**
Farmland	−0.07	0.92	−0.04	0.95
Woodland	−0.12	0.73	−0.22	0.35
Grassland	0.53	0.001	0.55	0.001
NP	0.06	0.51	0.04	0.59
AREA_MN	0.19	0.01	0.12	0.02
SHDI	0.26	0.09	0.21	0.15

GWR analysis and the results are shown in Figures 3 and 4. It can be seen from Figure 3 that the grassland landscape pattern index had a negative impact on the runoff of the URB in space, and the regression coefficients were all less than 0, but the negative impact on the runoff has regional differences. In 2000 and 2015, the average annual performance gradually decreases from north to south, indicating that the area with large grassland landscape had a more obvious impact on the runoff change. Combined with Figures 2 and 3, it can be seen that the grassland area in the northern region of the URB in 2015 was larger than that in 2000. Therefore, the negative influence degree in the northern region of the URB in 2015 was more serious than that in 2000.

As can be seen from Figure 4, the spatial non-stationary relationship between AREA_MN landscape pattern index and the regression coefficient of runoff was relatively complex, with a positive and negative influence staggered distribution, showing an obvious spatial pattern of north–south regional differentiation. In 2000 and 2015, the AREA_MN landscape pattern index in the northern URB had a positive influence on runoff, while in the southern URB it had a negative influence, and gradually weakened from north to south, indicating that the area with a large AREA_MN landscape index and a small degree of landscape fragmentation had a small influence on runoff change. According to Figures 2, 4 and 5, the higher the elevation of the URB in 2000 and 2015, the better the ecological environment, the lower the degree of landscape fragmentation, and the higher the runoff. It can also be seen that the landscape pattern index of the AREA_MN in the northern URB area had a better positive influence on runoff in 2000 than in 2015, indicating that the landscape fragmentation degree in this area was intensified from 2000 to 2015, thus influencing the formation and distribution of runoff.

DISCUSSION AND CONCLUSIONS

The main conclusions are as follows:

(1) Through sensitivity analysis and parameter calibration, the results show that the SWAT model had good applicability for runoff simulation of the URB under different land-use types in 2000 and 2015. The *Ens* coefficient and correlation coefficient R^2 of 2000 and 2015 annual rates in regular and validation periods met the requirements and can be used to study the impact of landscape pattern change on runoff.

(2) In 2000 and 2015, bare land was the main landscape type, accounting for 51.03% and 51.29% of the total

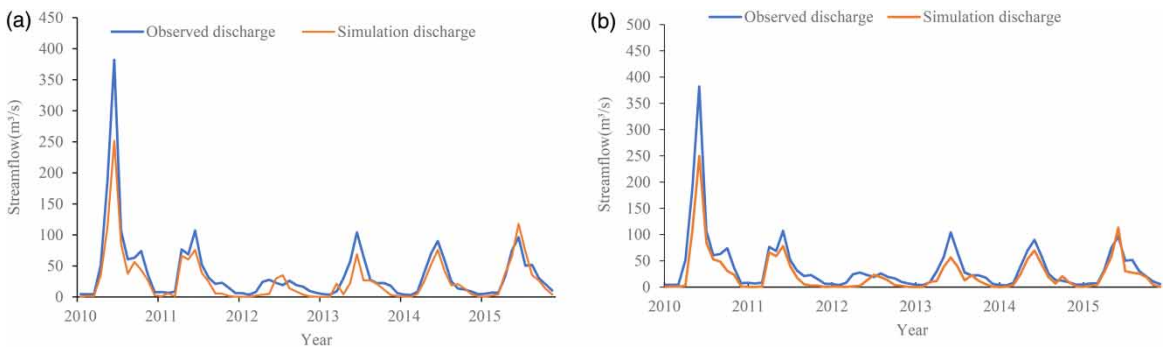

Figure 3 | Change process of runoff measured and simulated at the Ertai Hydrological Station under different land-use types in (a) 2000 and (b) 2010.

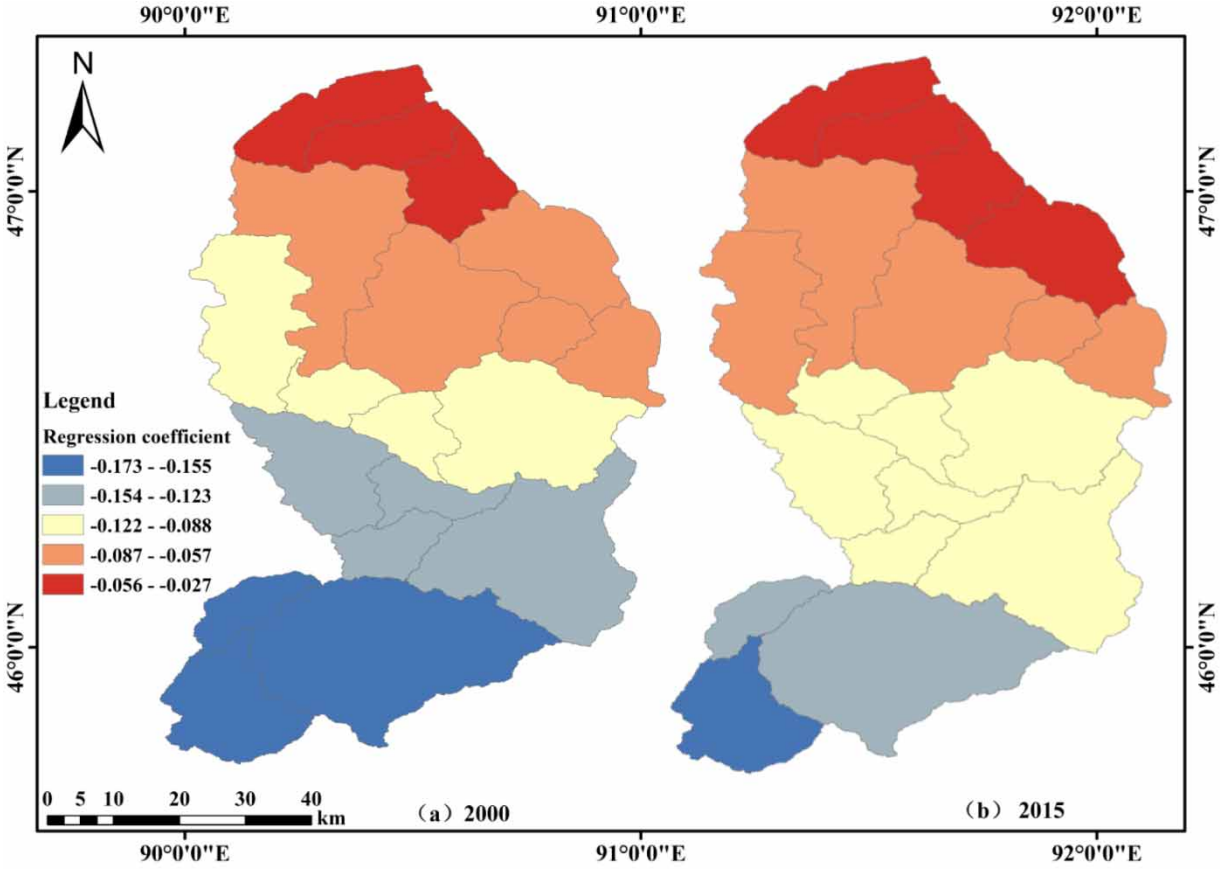

Figure 4 | Spatial pattern of regression coefficients in the GWR model for runoff and grassland landscape in the URB.

URB area, followed by grassland and woodland, accounting for 32.39% and 12.49% in 2000, respectively, and 32.75% and 11.30% in 2015, respectively. The proportions of cultivated land, water area, and construction land in the two periods were relatively small. During 2000–2015, the areas of woodland and grassland decreased, and the reduced area was mainly converted to bare land and cultivated land, while the other landscape types increased. Landscape index analysis at landscape level for the URB in 2000 and 2015 showed that the landscape in the study area was fragmented, landscape complexity increased, heterogeneity enhanced, and landscape patch connectivity decreased.

(3) The results of correlation analysis between runoff change and landscape pattern change show that the changes of woodland and grassland were positively correlated with runoff, while the changes of cultivated land, construction land, and bare land were negatively correlated with runoff. This indicates that the decrease of woodland and grassland area in 2000–2015 decreased the water conservation capacity of the study area, and the increase of cultivated land, construction land, and bare land area weakened the interception of precipitation at the surface and increases the infiltration capacity of precipitation, thus affecting the formation of runoff. The changes of LPI, AREA_MN, and CONTAG in landscape indices were positively correlated with runoff, while the changes of NP, PD, LSI, SHDI, and SHEI were negatively correlated with runoff. This indicates that in 2000–2015, the landscape fragmentation of the URB was aggravated, the landscape balance was destroyed and the connectivity was poor, which weakened the ability of rainfall interception and water conservation in the

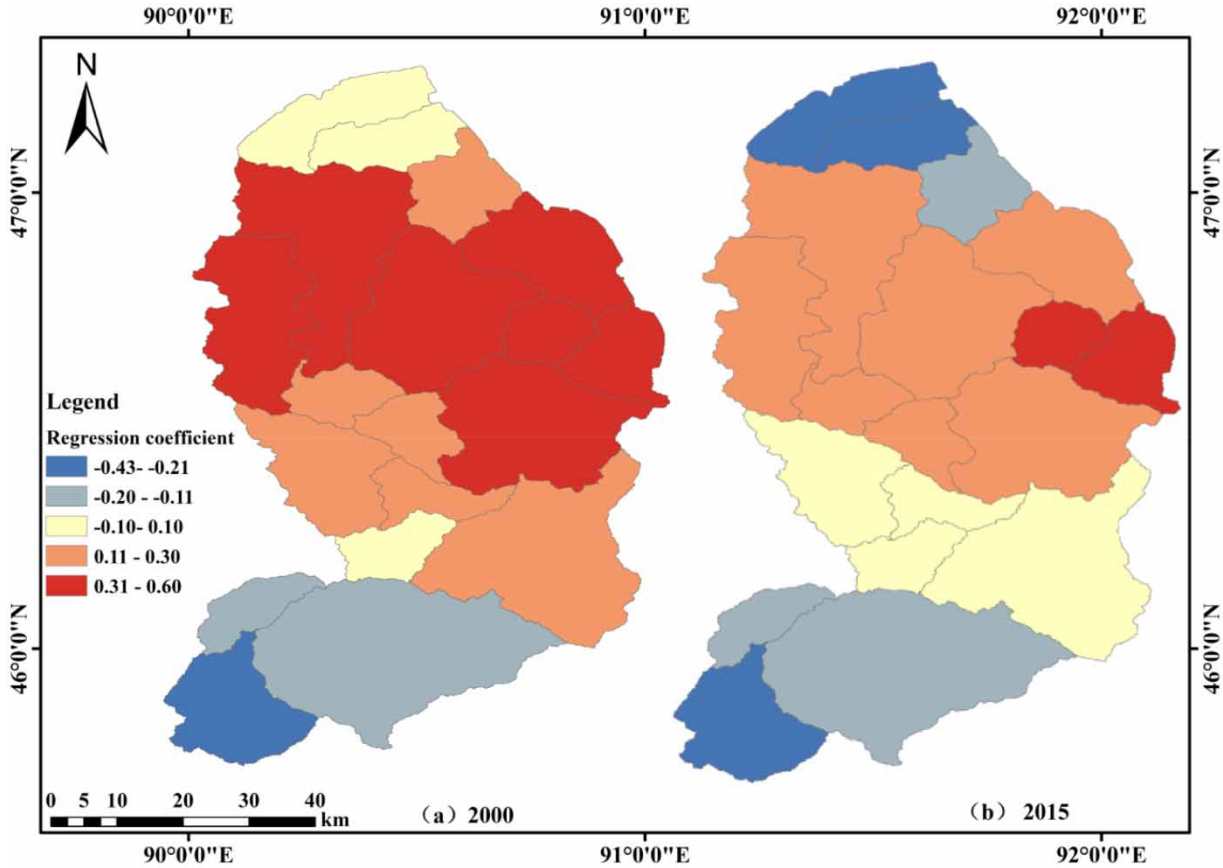

Figure 5 | Spatial pattern of regression coefficients in the GWR model of runoff and AREA_MN landscape index.

study area, and then affected the hydrological situation and runoff generation and confluence mechanisms in the study area.

(4) The results showed that the landscape pattern index of grassland had a negative impact on the runoff of the URB in space and had regional differences, which indicated that the area with more grassland landscape area had a more significant impact on the runoff change, and the negative impact in the northern region of the URB in 2015 was more serious than that in 2000. In 2000 and 2015, the AREA_MN landscape pattern index in the northern region of the URB had a positive impact on runoff, while in the southern region, it had a negative impact on runoff, and gradually weakened from north to south. This indicates that the areas with larger AREA_MN landscape index and smaller landscape fragmentation had less impact on runoff change, and the positive impact of AREA_MN landscape pattern index on runoff in the northern region of the URB in 2000 was better than that in 2015.

As the URB is located in the alpine and cold mountains, there are few meteorological stations and it is difficult to obtain observation data, which makes it difficult to build the meteorological database of the SWAT model in this type of watershed. Therefore, the meteorological data-driven SWAT model of CMADS established by Meng (2016) was adopted in this study. Compared with other atmospheric reanalysis data (such as ERA, JRA-25 Princeton data set, etc.), the CMADS data set was modified by nearly 40,000 regional automatic stations in China, which can better reflect the real meteorological characteristics of the near surface of China. Therefore, the advantages of the CMADS data set-driven SWAT model in simulating the runoff process were fully utilized in this study. By adjusting the parameters that have great influence on

runoff simulation, better simulation results can be achieved. At the same time, for different land-use types of the URB in 2000 and 2015, the SWAT model after parameter calibration not only fits the research objectives, but also meets the basic needs of this study. The GWR model was used to analysis the spatial correlation between different landscape pattern changes and runoff quantitatively in this paper, making up for the lack of analysis on the relationship between landscape index and runoff change characteristics in the study area.

FUNDING SUPPORT

1. The China National Natural Science Foundation Project no. 51769036.
2. Natural Science Foundation of Xinjiang Uygur Autonomous Region, China Project no. 2017D01A43.

REFERENCES

Brunsdon, C., Fotheringham, A. S. & Charlton, M. 1996 Geographically weighted regression: a method for exploring spatial nonstationarity. *Geographically Analysis* **28** (4), 281–298.

Dong, L., Xiong, L., Yu, K. & Li, S. 2012 Advances in the study of impacts of climate change and human activities on hydrology. *Advances in Water Science* **23** (2), 278–285.

Foley, J. A., DeFries, R., Asner, G. P., Barford, C., Bonan, G., Carpenter, S. R. & Helkowski, J. H. 2005 Global consequences of land use. *Science* **309** (5734), 570–574.

Gao, C., Zhai, J., Tao, H., Liu, B. & Su, B. 2009 Hydrological response to land use/land cover change in Chaohu basin. *Journal of Natural Resources* **24** (10), 1794–1902.

Ghaffari, G., Keesstra, S., Ghodousi, J. & Ahmadi, H. 2010 SWAT-simulated hydrological impact of land-use change in the Zanjanrood basin, Northwest Iran. *Hydrological Processes: An International Journal* **24** (7), 892–903.

Guo, L., Li, Y. & Guo, Z. 2018 Dynamic change analysis of land use and landscape pattern in Weibei Dry Highland of Baoji City. *Journal of Northwest Forestry College* **33** (5), 263–268.

He, B., Gao, F., Tang, X. & Qin, S. 2019 Diagnosis of hydrometeorological variability of arid inland rivers in Xinjiang based on sliding Copula function. *Soil and Water Conservation Research* **26** (1), 155–161.

Hou, W. & Gao, J. 2019 Based on SWAT model, the runoff service and its spatial variation of Sancha River ecosystem in Wujiang River were simulated. *Journal of Geographical Sciences* **29** (3), 432–448.

Kang, L., Bartel, B., Luo, N., Xue, Y. & Wang, M. 2018 Spatial and temporal variations and impacts of reference crop evapotranspiration at different time scales in Altay region. *Agrometeorology of China* **39** (8), 502–511.

Li, L., Jiang, D., Li, J., Liang, L. & Zhang, L. 2007 Advances in hydrological effects of land use/cover change. *Journal of Natural Resources* **22** (2), 211–224.

Li, Y., Luo, Y., Liu, G., Ou, Y. & Zheng, H. 2013 Effects of land use change on ecosystem services: a case study of Miyun Reservoir Basin. *Journal of Ecology* **33** (3), 726–736.

Lv, L., Zhang, J., Jiang, Y., Zheng, D. & Wang, X. 2018 Quantitative assessment of the impact of land use change on runoff yield process in the Dongjiang River Basin. *Water Resources Protection* **34** (3), 45–51.

Meng, X. 2016 *Land Component Simulation and Validation Based on Improved CLDAS-Driven CLM3.5 and SWAT Model*. Xinjiang University, Urumqi.

Meng, X., Shi, C., Liu, S., Wang, H., Lei, X., Liu, Z., Ji, X., Cai, S. & Zhao, Q. 2016 CMADS data set and its driving role in watershed hydrological model: a case study of Heihe River Basin. *People's Pearl River* **37** (07), 1–19.

Nurland, H. 2014 Hydrological characteristics of the Urengu River Basin. *Study on Arid Areas* **31** (5), 798–802.

Nurland, H., Shen, Y. & Mahathir, M. 2014 Impact of climate change on runoff processes in the Urengu River Basin, Altai Mountains. *Glacier Permafrost* **36** (3), 699–705.

Popov, E. G. 1979 *Gidrologicheskie prognozy (Hydrological Forecasts)*. Gidrometeoizdat, Leningrad.

Sriwongsitangon, N. & Taesombat, W. 2011 Effects of land cover on runoff coefficient. *Journal of Hydrology* **410** (3/4), 226–238.

Tian, Y., Zhang, M., Xu, D. & Zhang, S. 2019 Construction of ecological security pattern of urban landscape based on the theory of 'source-sink'. *Journal of Ecology* **39** (7), 2311–2321.

Wang, S., Zhang, Z., Sun, G., Zhang, M. & Yu, X. 2006 Hydrodynamic response of land use change in Loess Plateau Basin – taking Luergou Basin in Tianshui, Gansu Province as an example. *Journal of Beijing Forestry University* **28** (1), 48–54.

Wang, Y., Zhang, L. & Wang, J. 2016 Response of hydrological process to land use/cover change in Taohe River Basin. *Glacier Permafrost* **38** (1), 200–210.

Xu, Z. & Cheng, L. 2010 Research and application progress of distributed hydrological model. *Journal of Hydraulic Engineering* **41** (9), 1009–1017.

Yang, X. 2014 *Study on Water resoURBes Change in Wulungu River Catchment Area Based on SWAT Model*. Xinjiang Agricultural University, Urumqi.

Zhang, M. & Zeng, Y. 2018 Spatio-temporal dynamic changes and driving forces of wetland landscape in Changsha-Zhuzhou-Tan urban agglomeration. *Journal of Agricultural Engineering* **34** (1), 241–249.

First received 13 November 2019; accepted in revised form 2 February 2020. Available online 23 March 2020